Transmembrane Reorientation of the Substrate-Binding Site in Vesicular Acetylcholine Transporter†

Dawn T. Bravo, Natalia G. Kolmakova, and Stanley M. Parsons*

Department of Chemistry and Biochemistry, University of California, Santa Barbara, California 93106

Received January 20, 2004; Revised Manuscript Received April 11, 2004

ABSTRACT: Active transport of acetylcholine (ACh) by vesicular ACh transporter (VAChT) is driven by a proton-motive force established by V-ATPase. A published microscopic kinetics model predicts the ACh-binding site is primarily oriented toward the outside for nontransporting VAChT and toward the inside for transporting VAChT. The allosteric ligand [^{3}H]vesamicol cannot bind when the ACh-binding site is outwardly oriented and occupied by ACh, but it can bind when the ACh site is inwardly oriented. The kinetics model was tested in the paper reported here using rat VAChT expressed in PC12^{A1237} cells. Equilibrium titrations of [^{3}H]vesamicol binding and ACh competition show that ATP blocks competition between vesamicol and ACh in over one-half of the VAChT. NaCl did not mimic ACh chloride, and bafilomycin A_1 and FCCP completely blocked the ATP effect, which shows that it is mediated by a proton-motive force. The data are consistent with reorientation of over one-half of the ACh-binding sites from the outside to the inside of vesicles upon activation of transport. The observations support the proposed microscopic kinetics model, and they should be useful in characterizing effects of mutations on the VAChT transport cycle.

Vesicular acetylcholine transporter (VAChT)[1] translocates acetylcholine (ACh) from cytoplasm to the lumen of synaptic vesicles for evoked release from nerve terminals. Vesicular protons provided by V-ATPase are used by VAChT to power ACh transport. A "microscopic" kinetics model of the VAChT transport cycle (Figure 1) has been proposed (*1*−*3*). Microscopic in this context refers to the step-by-step mechanism. In the model, ligand-binding steps are assumed to be at equilibrium, whereas transmembrane reorientation steps for the ACh-binding site are described by rate constants. Estimates for the values of all microscopic parameters have been obtained for *Torpedo* VAChT. During accumulation of ACh, the net rate of the k_2' step (taking into account proton binding and back reaction) is much slower than that of the k_1' step and is thus rate-limiting. Computer simulation predicts that >98% of the ACh-binding site in nontransporting VAChT is outwardly oriented and ~99% of the ACh-binding site in transporting VAChT is inwardly oriented when external ACh is saturating and vesicles are empty.

Transport is potently inhibited by the compound (−)-*trans*-2-(4-phenylpiperidino)cyclohexanol (vesamicol), which binds to an allosteric site on the outside of VAChT (*4*, *5*) to form at least two types of the dead-end complex, one with the ACh-binding site facing outside and one facing the inside (Figure 1). When external ACh binds to outwardly oriented transporter, vesamicol cannot bind (*1*). External ACh presumably cannot bind to inwardly oriented transporter because the ACh-binding site is not exposed. The studies reported here tested whether transport-dependent changes in exposure of the ACh-binding site can be detected based on the ability of external ACh to compete with [^{3}H]vesamicol for binding.

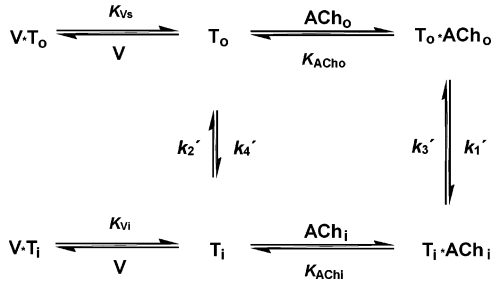

FIGURE 1: Microscopic kinetics model of the VAChT transport cycle and vesamicol binding. Proceeding in the clockwise direction, T_o binds ACh_o with equilibrium dissociation constant K_{ACh_o} and reorients in step k_1' to expose bound ACh to the inside of the vesicle. ACh_i is then released with the dissociation constant K_{ACh_i}. T_i reorients in step k_2' to expose the empty ACh-binding site to the outside and to complete a cycle. The primes indicate that the rate constants are pH-dependent. The compound vesamicol binds to an allosteric site on the outside of T_o and T_i. It cannot bind T_oACh_o.

MATERIALS AND METHODS

The cDNA for rat VAChT was obtained as a generous gift from A. Roghani (Lubbock, TX). The PC12^{A1237} cell line, derived from PC12 cells commonly used as a neurosecretory model system, was obtained as a generous gift from

† This research was supported by Grant NS15047 from the National Institute of Neurological Disorders and Stroke.

* To whom correspondence should be addressed. Phone: (805) 893-2252. Fax: (805) 893-4120. E-mail: parsons@chem.ucsb.edu.

[1] Abbreviations: VAChT, vesicular acetylcholine transporter; ACh, acetylcholine; vesamicol, (−)-*trans*-2-(4-phenylpiperidino)cyclohexanol; B_{max}, maximal binding at saturating concentration of vesamicol; K_v, vesamicol dissociation constant; HEPES, 4-(2-hydroxyethyl)-1-piperazineethanesulfonic acid; UBB, uptake-binding buffer (110 mM potassium tartrate, 20 mM HEPES, and 1 mM ascorbic acid adjusted to pH 7.4 with KOH); UBB/P, uptake-binding buffer containing 100 μM diethyl-*p*-nitrophenyl phosphate; FCCP, carbonyl cyanide *p*-(trifluoromethoxy)phenylhydrazone.

10.1021/bi049846w CCC: $27.50
Published on Web 06/17/2004

L. B. Hersh (Lexington, KY). It expresses negligible endogenous VAChT (*6*). Expression vector pcDNA3.1D/V5-His-TOPO, One Shot TOP10 chemically competent *Escherichia coli* cells, synthetic oligonucleotide primers 5′-CACCATGGAACCCACCGCGCC-3′ and 5′-CTAGCTGCGGGAGTAATAGTTGTAGTCG-3′, Dulbecco's modified Eagle's medium (DMEM)/Ham's F12 (1:1) mixture, phosphate-buffered saline (PBS) at pH 7.4 (PBS) (without $CaCl_2$ and $MgCl_2$), trypsin-EDTA, and penicillin (10 000 units/mL)/streptomycin sulfate (10 000 μg/mL) were supplied by Invitrogen Corp. (Carlsbad, CA). ACh chloride, (−)-vesamicol·HCl, carbonyl cyanide *p*-(trifluoromethoxy)phenylhydrzone (FCCP), sodium dodecyl sulfate, ATP magnesium salt, L-(+)-tartaric acid dipotassium salt, L-(+)-tartaric acid disodium salt, polyethylenimine, 0.4% trypan blue in PBS, diethyl-*p*-nitrophenyl phosphate, phenylmethylsulfonyl fluoride, and fetal bovine serum were obtained from Sigma−Aldrich Chemical Corporation (St. Louis, MO). Luria−Bertani medium was obtained from Becton, Dickinson, and Company (Cocksville, MD). Plasmid purification kit was obtained from Qiagen (Valencia, CA). [^{3}H]Vesamicol (30−60 Ci/mmol) and [acetyl-^{3}H]ACh iodide (50−100 mCi/mmol) were obtained from Perkin−Elmer Life Sciences Inc. (Boston, MA). [^{3}H]ACh was diluted to one-third of the commercial specific radioactivity with nonradioactive ACh. Electrode gap cuvettes (0.4 cm) were obtained from Bio-Rad Laboratories (Hercules, CA). Equine serum was obtained from HyClone (Logan, UT). Complete protease inhibitor cocktail tablets were obtained from Roche (Mannheim, Germany). A 50-fold concentrated stock solution of protease inhibitors was obtained by dissolving one tablet into 1 mL of H_2O. Glass microfiber filter circles GF/F (1.3 cm) were obtained from Whatman International Ltd. (Maidstone, England). Scintillation cocktail (Bio-Safe II) was obtained from Research Products International Corporation (Mount Prospect, IL). A DNA-sequencing kit (Thermo Sequenase) was obtained from USB Corp. (Cleveland, OH). All other materials and reagents were obtained from usual commercial sources.

Rat VAChT cDNA was amplified using synthetic oligonucleotide primers (see above) by polymerase chain reaction. The purified DNA was ligated directionally into linearized pcDNA 3.1 expression vector, thus creating a circular pcDNA 3.1/VAChT recombinant vector. *E. coli* One Shot TOP10 competent cells were transformed with recombinant vector by heat shock and plated onto Luria−Bertani agarose plates containing ampicillin (100 μg/mL). Clones were grown in Luria−Bertani medium containing ampicillin, and vector DNA was isolated using the Qiagen purification kit. Sequence analysis of the recombinant vector using the Thermo Sequenase kit confirmed that the rat VAChT coding sequence was intact and correctly inserted. Cells carrying the confirmed vector were grown at 37 °C in Luria−Bertani medium containing ampicillin for amplification.

Rat VAChT was expressed as described with minor variations (*5*, *7*). PC12$^{A123.7}$ cells were cultured at 37 °C in 10% CO_2 in a complete medium DMEM/Ham's F12 (1:1) mixture containing 10% fetal bovine serum, 5% horse serum, penicillin (100 units/mL), and streptomycin (100 μg/mL). Electroporation was performed to transfect PC12$^{A123.7}$ cells with pcDNA 3.1/VAChT recombinant vector. Cells detached by trypsin/EDTA were washed twice in ice-cold PBS at pH 7.4. They were resuspended in 800 μL of ice-cold PBS at a concentration of $\sim 6 \times 10^7$ cells/mL. Resuspended cells were mixed with pcDNA 3.1/VAChT (50−75 μg) and incubated on ice for 10 min. The cell mixture was placed into chilled 0.4-cm gap cuvettes and electroporated at 0.2 kV and 1400 microfarads. Electroporated cells were plated in complete media and cultured for ~72 h, changing media as required.

Rat VAChT expressed in PC12 cells localizes primarily to synaptic-like microvesicles (*5*, *8*). To prepare postnuclear supernatant containing microvesicles, cultured cells were detached with trypsin/EDTA and washed twice with 30 mL of cold PBS by gentle centrifugal pelleting. Washed cells were resuspended in a homogenization buffer composed of 0.32 M sucrose and 10 mM HEPES adjusted to pH 7.4 with KOH and also containing 0.1 mM phenylmethylsulfonyl fluoride and the recommended concentration of the manufacturer of complete protease inhibitor cocktail. Resuspended cells were placed in a motor-driven Potter−Elvejhem homogenizer with a tight-fitting pestle, and they were homogenized at medium speed to ~90% breakage (~3−6 strokes). Breakage was assessed by mixing cells (10^6 per mL) with an equal volume of trypan blue in PBS. Dyed cells were allowed to incubate at 23 °C for 1−2 min, after which they were placed in a hemocytometer and viewed with a 10× objective. Homogenized cells were centrifuged at 800*g* for 10 min. The postnuclear supernatant was collected, and the protein content was determined by the method of Bradford (*9*). The postnuclear supernatant was stored at −80 °C until used. After the postnuclear supernatant was thawed, it was treated with 100 μM diethyl-*p*-nitrophenyl phosphate at 23 °C for 30 min to inhibit ACh esterase. All experiments were at 37 °C, and all solutions were prewarmed before initiating reaction. All reactions were incubated 10 min unless indicated otherwise. When ATP was present, the final concentration was 5 mM, and 2 mM final concentration of $MgCl_2$ was also present.

The filter assay for bound [^{3}H]ACh or [^{3}H]vesamicol was conducted as follows (*7*). Incubation was terminated by mixing a 90-μL portion of the suspension with a 1-mL portion of ice-cold uptake binding buffer (UBB) composed of 110 mM potassium tartrate, 1 mM ascorbic acid, and 20 mM HEPES adjusted to pH 7.4 with KOH. The diluted suspension was rapidly and quantitatively filtered with vacuum assistance through a polyethylenimine-coated glass microfiber filter circle GF/F (1.3 cm) prewetted with UBB, after which the filter immediately was washed with vacuum assistance by three 1-mL portions of ice-cold UBB. Damp filters were transferred to a liquid scintillation vial. For [^{3}H]-ACh, 350 μL of 1% (w/v) sodium dodecyl sulfate was added and the vial was incubated 30−60 min to fully solubilize ACh. For both [^{3}H]ACh and [^{3}H]vesamicol, 3.5 mL of scintillation cocktail was added and radioactivity was determined by liquid scintillation counting. Nonspecific uptake of radioligand was determined in a similar manner in 4 μM unlabeled vesamicol (except as noted). Specific uptake is the difference between total (absence of unlabeled vesamicol) and nonspecific uptake. All experiments were conducted in duplicate, and data were averaged. Averaged data were fit by nonlinear regression using appropriate equations, and error estimates of one standard deviation are given. Error estimates are propagated.

Transport of [^{3}H]ACh was measured as described (5) with minor modifications. Postnuclear supernatant (50 μL) containing 200 μg of protein was mixed with 50 μL of UBB also containing 100 μM diethyl-*p*-nitrophenyl phosphate (UBB/P). Uptake was initiated by the addition of 100 μL of UBB/P containing 10 mM ATP, 4 mM $MgCl_2$, and twice the final concentration of [^{3}H]ACh.

The saturation curves for [^{3}H]vesamicol binding were determined by mixing postnuclear supernatant (100 μL) containing 100 μg of protein with 100 μL of UBB/P containing 10 mM ATP, 4 mM $MgCl_2$, and/or 400 mM ACh and twice the indicated final concentration of [^{3}H]vesamicol.

Competition of ligands with [^{3}H]vesamicol in the absence and presence of ATP was studied by mixing postnuclear supernatant (50 μL) containing 200−400 μg of protein with 100 μL of UBB/P containing twice the indicated final concentration of unlabeled competitor (ACh chloride or NaCl). Either 50 μL of UBB/P containing 20 nM [^{3}H]-vesamicol or 50 μL of UBB/P containing 20 nM [^{3}H]-vesamicol, 20 mM ATP, and 8 mM $MgCl_2$ was added and mixed well. This resulted in a 5 nM final concentration of [^{3}H]vesamicol.

Time dependence of [^{3}H]vesamicol binding and exchange was studied by mixing postnuclear supernatant (50 μL) containing 225 μg of protein with 100 μL of UBB/P containing 10 nM [^{3}H]vesamicol and no other ligand or 400 mM ACh. The reaction was initiated by addition of 50 μL of UBB/P or UBB/P containing 20 mM ATP and 8 mM $MgCl_2$ and allowed to proceed for the indicated times. At 5.5 min, a similar suspension was brought to 4 μM in nonradioactive vesamicol and allowed to exchange for the indicated times.

The effects of bafilomycin A_1 and FCCP on binding of [^{3}H]vesamicol were determined by mixing postnuclear supernatant (50 μL) containing 200−400 μg of protein with 100 μL of UBB/P containing 0 or 400 mM unlabeled ACh and twice the indicated final concentration of bafilomycin A_1 or FCCP. The suspension was incubated for 15−30 min. Vesamicol-binding competition was initiated by addition of 50 μL of UBB/P containing 20 nM [^{3}H]vesamicol, 20 mM ATP, and 8 mM $MgCl_2$.

RESULTS

Expressed rat VAChT was confirmed to transport [^{3}H]-ACh (Figure 2). All transport is due to VAChT, because an insignificant amount of specific transport was present in postnuclear supernatant prepared from cells transfected with the vector not carrying cDNA for VAChT (not shown). Transport was normalized to the amount of VAChT using the maximal amount of specifically bound [^{3}H]vesamicol (B_{max}) in the absence of other ligands. The first 5% or so of transport was too little relative to the amount of nonspecific binding to accurately determine the initial velocity. Thus, transport was allowed to proceed beyond the initial period to collect data. Nevertheless, the measured rate behavior exhibits apparent Michaelis−Menten properties, and fitted parameters will be in error only slightly. They were V_{max}/B_{max} equal to 10.4 ± 0.3 min^{-1} and K_m equal to 0.50 ± 0.05 mM ACh. The result demonstrates that the preparation is functional. However, the data in Figure 2 do not determine what fraction of expressed VAChT is functional.

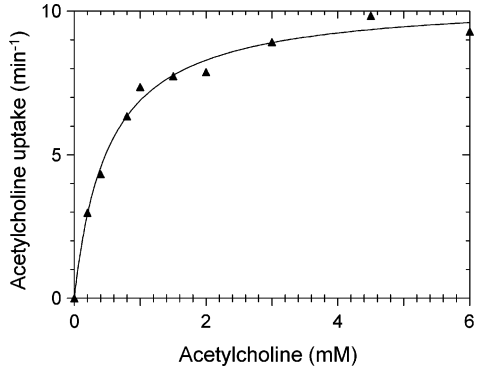

FIGURE 2: Active transport of ACh by expressed VAChT. Transport was carried out as described in the Materials and Methods in the indicated concentrations of [^{3}H]ACh. The rate of ACh uptake (min^{-1}) was obtained by dividing specific transport (pmol ACh mg^{-1} min^{-1}) at each concentration of [^{3}H]ACh by B_{max} (pmol VAChT/mg) determined for the same preparation of membranes. A rectangular hyperbola was fit to the transformed data to generate the curve shown.

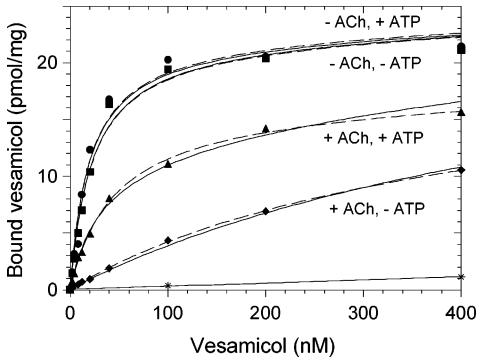

FIGURE 3: [^{3}H]Vesamicol binding curves. VAChT was incubated in the indicated concentrations of [^{3}H]vesamicol with no other ligand (■), 5 mM ATP (●), 5 mM ATP plus 200 mM ACh (▲), 200 mM ACh (◆), or 40 μM unlabeled vesamicol (*). Appropriate equations that assumed either independent B_{max} values (- - -) or the same B_{max} value for all conditions (—) were fit to the data. Estimates of parameter values for the two models are listed in Table 1.

ATP and ACh Greatly Affect [^{3}H]Vesamicol-Binding Curves. Almost all specific binding of [^{3}H]vesamicol is due to VAChT, because only a very small amount was present in the postnuclear supernatant prepared from cells transfected with the vector not carrying cDNA for VAChT (not shown). Data for binding of low to high concentrations of [^{3}H]-vesamicol were obtained in the absence or presence of essentially saturating concentrations of ATP and/or ACh. The different conditions caused very substantial changes in the data obtained (Figure 3 and Table 1).

Two models were tested for analysis of the saturation data. In the first model, B_{max} values were assumed to be independent of each other. A rectangular hyperbola (added to linear nonspecific binding) was fit independently to the set of data obtained for each condition. ATP had no significant effect on affinity (K_v = 20.0 ± 2.0 nM) or maximal binding (B_{max} = 22.5 ± 0.6 pmol/mg) compared to the values in the absence of other ligands (K_v = 22.6 ± 2.3 nM and B_{max} = 22.3 ± 0.7 pmol/mg). ACh decreased apparent affinity 15-fold (K_v = 349 ± 181 nM) because of allosteric competition with vesamicol, and it decreased maximal binding about 25% (B_{max} = 17.6 ± 5.2 pmol/mg). Addition of ATP to ACh increased apparent affinity 8-fold (K_v = 44.7 ± 7.5 nM) with

Table 1: Effects of Other Ligands on Binding of [^{3}H]vesamicol to VAChT[a]

	constant total B_{max}[b]		conditional B_{max}[c]		competition measurements		
other ligands	B_{max} (pmol/mg)	K_v[d] (nM)	B_{max} (pmol/mg)	K_v[d] (nM)	K_{ACh}[e] (mM)	nondisplaceable[e] (pmol/mg)	k_{off}[f] (min^{-1})
none	22.4 ± 0.5	22.4 ± 2.0[g]	22.3 ± 0.7	22.6 ± 2.3	16.1 ± 1.7	0.08 ± 0.04	0.13 ± 0.01
ATP	11.4 ± 1.4[h]	17.5 ± 2.8[i]	22.5 ± 0.6	20.0 ± 2.0	16.1 ± 1.7	0.62 ± 0.04	0.26 ± 0.01
nr	11.0 ± 1.4[j]	22.4 ± 2.0[g]					
ACh	22.4 ± 0.4	524 ± 55[k]	17.6 ± 5.2	349 ± 181			0.16 ± 0.03
ATP + ACh	11.4 ± 1.4[h]	28.3 ± 7.6[i]	16.2 ± 0.9	44.7 ± 7.5			0.35 ± 0.02
nr	11.0 ± 1.4[j]	524 ± 55[k]					

[a] Parameter values obtained from fits to the data shown in Figures 3−5. [b] Total B_{max} values for all ligand conditions were assumed to be the same in fitting Figure 3. [c] B_{max} values for different ligand conditions were assumed to be independent of each other in fitting Figure 3. [d] K_v values are apparent and do not correlate directly with K_{vs} and K_{vi} in Figure 1. [e] Equilibrium ability of ACh to displace trace bound [^{3}H]vesamicol, taken from Figure 4. [f] Rate of replacement of trace bound [^{3}H]vesamicol with unlabeled vesamicol, taken from Figure 5. [g] Assumes K_v values for VAChT not responding to ATP and "none" are the same. [h] Assumes the same amount of VAChT responds to ATP in ATP alone and ATP plus ACh. [i] Assumes VAChT responding to ATP has independently adjustable K_v value that can be different for T_o (ATP alone) and T_i (ATP plus ACh) species in Figure 1. [j] Assumes amount of VAChT not responding to ATP is the same in ATP or ATP plus ACh. [k] Assumes apparent low-affinity binding in ACh alone and apparent low-affinity binding not responding in ATP plus ACh have the same K_v value.

no significant change in the maximal binding (B_{max} = 16.2 ± 0.9 pmol/mg) relative to the values in ACh alone.

In the second model, B_{max} was assumed to have the same value under all conditions. A global, simultaneous fit to the data sets, incorporating the considerations listed below, resulted in a B_{max} value of 22.4 ± 0.5 pmol/mg. Binding of vesamicol in the absence of other ligands was assumed to be monophasic. It exhibited high affinity (K_v = 22.4 ± 2.0 nM). Binding of vesamicol in ACh also was assumed to be monophasic, but it exhibited 23-fold lower apparent affinity (K_v = 524 ± 55 nM) because of allosteric competition. Addition of ATP to ACh converted somewhat more than one-half of the transporter (11.4 ± 1.4 pmol/mg) from apparent low to high affinity (K_v = 28.3 ± 7.6 nM), requiring a biphasic fit to that set of data. The remainder of the VAChT was assumed to exhibit low apparent affinity because it did not sense the presence of ATP. It also was assumed that (i) VAChT responding to ATP in the presence of ACh might respond to ATP in the absence of ACh to change K_v and (ii) the remainder of the VAChT in ATP (and no ACh) had the same value of K_v as in the absence of other ligands because it did not sense ATP. Thus, a biphasic fit to the set of data obtained in ATP was implemented. The estimated affinity of the binding sites responding to ATP (K_v = 17.5 ± 2.8 nM) is not significantly different from that of VAChT in the absence of other ligands (K_v = 22.4 ± 2.0 nM). Nevertheless, results presented below consistently show that ATP causes slightly more binding of trace [^{3}H]vesamicol, which in agreement with the results of the biphasic fit suggests that ATP slightly increases vesamicol affinity. The estimated affinity of the tighter binding sites in ATP plus ACh is not significantly different from that of the tighter binding sites in ATP alone (K_v = 28.3 ± 7.6 versus 17.5 ± 2.8 nM).

Both models indicate that ATP decreases competition between ACh and [^{3}H]vesamicol manyfold. However, the second model is consistent with our knowledge about the vesamicol-binding site, which remains on the outside during transport and is not known to be labile (*1, 10*). The sum of the squares of fitting errors was slightly smaller for the first model, but that fit used two more adjustable parameters than that for the second model. Although the second model might seem more complicated, it actually is simpler in the sense of using fewer adjustable parameters and thus is preferred statistically. Moreover, the second model provides an explanation for other observations reported here that the first model does not. Thus, the model assuming constant B_{max} was adopted for the remainder of the analysis. The discussion presents a hypothesis to explain why some expressed VAChT does not sense ATP.

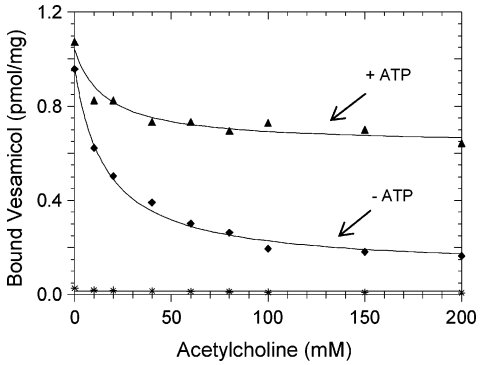

FIGURE 4: Competition of ACh with trace [^{3}H]vesamicol. VAChT was incubated in 5 nM [^{3}H]vesamicol and the indicated concentrations of ACh with no other ligand (◆), 5 mM ATP (▲), or 4 μM unlabeled vesamicol (*). Hyperbolic displacement equations having the same K_{ACh} value were fit to the data simultaneously to determine a K_{ACh} value of 16.1 ± 1.7 mM. Nonspecific binding was 0.01 pmol/mg. In the absence of ATP, the *y* intercept was 0.95 ± 0.02 pmol/mg, and the amount of [^{3}H]vesamicol displaced at infinite ACh was 0.86 ± 0.03 pmol/mg, leaving 0.08 ± 0.04 pmol/mg of specific binding not displaced. In ATP, the *y* intercept was 1.03 ± 0.02 pmol/mg, and the amount of [^{3}H]vesamicol displaced at infinite ACh was 0.40 ± 0.03 pmol/mg, leaving 0.62 ± 0.04 pmol/mg of specific binding not displaced. Fitted values are summarized in Table 1.

ATP Greatly Affects ACh Competition Curves. A trace concentration of [^{3}H]vesamicol was used to monitor the ability of ACh to displace vesamicol ± ATP (Figure 4 and Table 1). The use of trace [^{3}H]vesamicol minimizes a competition-dependent increase in the apparent dissociation constant for ACh. The assay assumes all [^{3}H]vesamicol binding is dynamic and responsive to the status of VAChT (see below for tests of this assumption). In the absence of ACh (read data on the *y* axis), slightly more [^{3}H]vesamicol was bound in ATP. In the absence of ATP, saturating ACh (as extrapolated by regression) displaced 91 ± 4% of bound [^{3}H]vesamicol with an equilibrium K_{ACh} value of 16.1 ± 1.7 mM. In ATP, saturating ACh displaced only 39 ± 8% of bound [^{3}H]vesamicol. In this experiment, ATP increased the amount of nondisplaceable [^{3}H]vesamicol some 8-fold. The

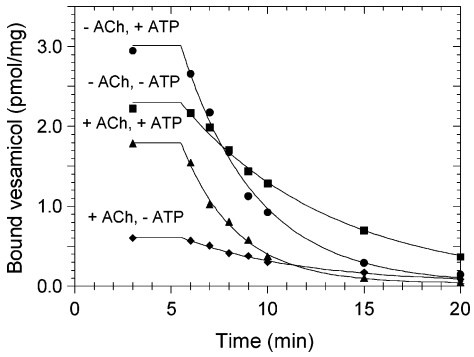

FIGURE 5: Dissociation rates for [^{3}H]vesamicol. VAChT was incubated with 5 nM of [^{3}H]vesamicol and no other ligand (■), 5 mM ATP (●), 5 mM ATP plus 200 mM ACh (▲), or 200 mM ACh (◆). Unlabeled vesamicol (4 μM) was added at 5.5 min to initiate exchange. Nonspecific binding was subtracted from the data before plotting. Fitted rate constants are given in Table 1.

result suggests that the number of available ACh-binding sites decreased substantially in ATP.

[^{3}H]Vesamicol Binding Is at Equilibrium. Vesamicol binding should be independent of time if it is at equilibrium. The amounts of bound trace [^{3}H]vesamicol in fact were nearly constant for more than 20 min under all conditions, and somewhat more [^{3}H]vesamicol was bound in ATP compared to no ATP (not shown). Binding also should be reversible if it is at equilibrium. A large excess of unlabeled vesamicol was added after incubation for 5.5 min in [^{3}H]-vesamicol to test this. Bound [^{3}H]vesamicol declined in first-order processes to the level of nonspecific binding (as extrapolated by regression) under all conditions, apparently because of the exchange that was rate-limited by dissociation (Figure 5). In all other experiments reported here, other ligands were added before or simultaneously with [^{3}H]-vesamicol to avoid prolonged reequilibration periods implied by the relatively slow rates shown in Figure 5.

ATP increased the dissociation rate constant (k_{off}) about 2-fold whether or not ACh was present (Table 1). Despite clearly biphasic equilibrium titration for vesamicol binding in ATP plus ACh, the dissociation process under this condition was monophasic. The behavior is expected for a competitive relationship between ACh and vesamicol in which no ternary complex (namely, $V{\cdot}T_o{\cdot}ACh_o$) exists. Also, probable biphasic binding in ATP alone showed monophasic dissociation. However, the two equilibrium affinities under this condition differ so little from each other that it is not surprising the corresponding dissociation processes do not resolve from each other experimentally. Overall, binding of vesamicol under all conditions is dynamic, and all bound [^{3}H]vesamicol is inherently dissociable.

ACh Competition Is Specific. A high concentration of ACh also involves a high concentration of counterion, in this case chloride, and high ionic and osmotic strengths. The possibility that the effects illustrated in Figures 3 and 4 are dependent on one of these other factors and not ACh was tested by repeating the competition experiment using NaCl instead of ACh chloride. Again, somewhat more trace [^{3}H]-vesamicol was bound in ATP compared to the absence of other ligands. A value of 0−200 mM NaCl did not affect the amounts of bound [^{3}H]vesamicol under both conditions (not shown). The result means that the phenomena observed in this paper are properties of ACh and not chloride or high ionic and osmotic strengths.

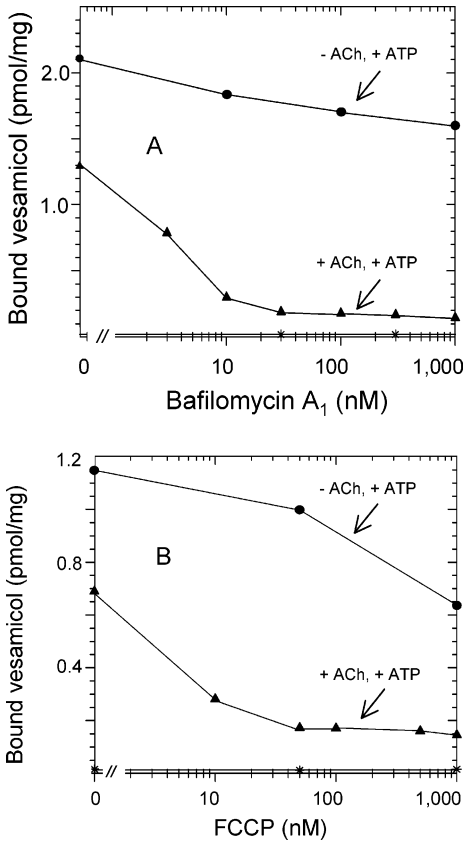

FIGURE 6: Effects of blocking the proton-motive force. VAChT was incubated with 5 nM [^{3}H]vesamicol, 5 mM ATP, and no other ligand (●), 200 mM ACh (▲), or 4 μM vesamicol (*) in the indicated concentrations of bafilomycin A_1 (A) or FCCP (B).

Bafilomycin A_1 and FCCP Block ATP Control of ACh Competition. The results to this point demonstrate that ATP controls competition between vesamicol and ACh. One possible mediator of the control is the proton-motive force generated by V-ATPase. Another possibility is protein kinase or an unknown activity.

The origin of ATP control was tested with bafilomycin A_1 (Figure 6A), which is a very potent and selective inhibitor of V-ATPase (*11*). All samples contained ATP. In the absence of bafilomycin A_1, binding of trace [^{3}H]vesamicol was 40% less in essentially saturating ACh than that in the absence of ACh (read data on the *y* axis), which is in agreement with Figure 3. In the presence of ACh, as little as 30 nM bafilomycin A_1 caused over a 90% loss of [^{3}H]-vesamicol binding. In the absence of ACh, this concentration of bafilomycin A_1 caused only a slight loss of binding, which is consistent with slightly lower affinity for [^{3}H]vesamicol because of the blockade of ATP action. In this experiment, ATP increased the amount of bound [^{3}H]vesamicol resistant to displacement by ACh some 10-fold (compare binding in absence and presence of bafilomycin A_1).

FCCP collapses the proton-motive force by catalyzing electrogenic movement of protons across membranes (*12*). Thus, it should have effects similar to those of bafilomycin A_1 if the ATP effect is due to the generation of the proton-motive force. All samples contained ATP (Figure 6B). In the absence of FCCP, binding of trace [^{3}H]vesamicol again was 40% less in essentially saturating ACh (read data on

the *y* axis). In the presence of ACh, as little as 50 nM FCCP caused nearly a complete loss of [^{3}H]vesamicol binding. In the absence of ACh, this concentration of FCCP caused only a slight loss of binding, which again is consistent with slightly lower affinity for [^{3}H]vesamicol because of the blockade of ATP action. Higher concentrations of FCCP inhibited binding more, possibly because of the disruption of the membrane structure. In this experiment, ATP increased the amount of bound [^{3}H]vesamicol resistant to displacement by ACh some 11-fold (compare binding in absence and presence of FCCP).

At low concentrations most likely to act specifically, bafilomycin A_1 and FCCP had very similar effects on the binding of [^{3}H]vesamicol. The results demonstrate that the proton-motive force protects the binding of [^{3}H]vesamicol from competition by ACh.

DISCUSSION

The kinetic K_m and equilibrium K_{ACh} values determined in Figures 2 and 4 of 0.50 and 16 mM, respectively, are similar to those previously reported for VAChT by other researchers (*3*, *5*, *13*−*16*). The observation that K_m and K_{ACh} values differ from each other does not indicate the existence of two types of binding sites for ACh. The values differ because the uptake of bound ACh by the k_1' step is faster than the return of the empty ACh-binding site to the outside by the k_2' step (Figure 1). The kinetics effect causes the apparent affinity of transported ACh to increase, but the thermodynamic affinity is unchanged.

Before proceding to interpretation of the results, critical observations that simplify the task are listed. [^{3}H]Vesamicol binding is at equilibrium under all conditions, which means that it will reliably report changes in the status of VAChT. The effects of ACh chloride are due to ACh and not chloride or high ionic and osmotic strengths. For K_{ACh} equal to 16 mM, about 93% of exposed ACh-binding sites are occupied at 200 mM ACh. For simplicity, all exposed sites are assumed to be occupied in 200 mM ACh. Only 15−20% of the vesamicol-binding sites are occupied when 5 nM "trace" [^{3}H]vesamicol is used in an experiment. Because most of the VAChT is not bound to vesamicol, most of the transporter can transport if it has an available proton-motive force and ACh. Finally, ATP acts on VAChT through the proton-motive force and not phosphorylation or another mechanism. The absence of any high-affinity component in the saturation curve for [^{3}H]vesamicol in ACh (Figure 3) means that no residual proton-motive force was present in microvesicles not exposed to added ATP. Also, because this cell line contains almost no choline acetyltransferase, it contains almost no ACh and endogenous ACh cannot complicate the observed behavior (*6*).

The simplest explanation for the observations is that somewhat more than one-half of expressed VAChT reorients its ACh-binding site from the outside to the inside when ACh transport is activated. Whether transported ACh binds to inwardly oriented VAChT is not known, but it apparently does not inhibit vesamicol binding as well as external ACh.

The ACh-binding site that does not face inside under transport conditions could arise from at least two sources. The first is the steady-state fraction of the site that faces outside during a transport cycle. In computer simulations, this is a very small fraction for empty vesicles exposed to saturating ACh, but it rises toward 1 as the vesicles fill with ACh because the rate of the k_3' step increases (*2*). It is not known how full the vesicles became in these experiments. A second source of outwardly facing ACh-binding site is VAChT in membranes not generating a proton-motive force. This could occur in several ways. Overexpressed VAChT is present in numerous membrane compartments because subcellular trafficking is overloaded (*17*, *18*). Compartments such as endoplasmic reticulum do not generate a significant proton-motive force. Using immunocytochemistry, the presence of VAChT in membranes not containing the vesicular marker synaptophysin was confirmed (not shown). Also, homogenization during preparation of the postnuclear supernatant might break open vesicles or shear V-ATPase off the vesicular membrane. In separate experiments, over homogenization of the preparation destroyed transport but left vesamicol binding intact (not shown). Synaptic vesicles isolated from *Torpedo* electric organ and chromaffin granules isolated from adrenal medulla clearly exhibit variable transport because of the damage during isolation (*3*). Although breakage of cells during homogenization was carefully monitored in the current paper to optimize the yield and functionality of VAChT, definite assurance that microvesicles were not damaged is unavailable.

These unknowns mean that the fractions of the outwardly and inwardly oriented ACh-binding site in transporting VAChT cannot be determined from available data. Nevertheless, it is clear that more than one-half of the ACh-binding sites changed from outward to inward orientation when transport was activated.

The following mechanistic model is consistent with the observations. In the presence of the proton-motive force and trace [^{3}H]vesamicol, a molecule of VAChT *not bound to vesamicol* binds and transports a molecule of ACh. The same molecule of VAChT then binds [^{3}H]vesamicol. For as long as the ACh-binding site faces inside, a *second* molecule of outside ACh is unable to bind and prevent binding of [^{3}H]-vesamicol. The result is more binding of [^{3}H]vesamicol during steady-state transport than during rest. The model generates measurable protection of [^{3}H]vesamicol binding from saturating ACh if the net rate of the k_1' step is (i) less than that of the k_2' step in nontransporting VAChT and (ii) more than that of the k_2' step in transporting VAChT. Such relative rates in fact are predicted by the proposed kinetics model (*1*−*3*).

Intrinsic affinity for vesamicol changes only a little for resting (no proton-motive force and no ACh), energized (presence of a proton-motive force but no ACh), and transporting VAChT (presence of a proton-motive force and ACh). This behavior is remarkable, because these conditions encompass major changes in transmembrane gradients, transporter dynamics, and orientation of the ACh-binding site. Furthermore, a minimal equilibrium response by vesamicol binding hides an interesting kinetics phenomenon. ATP increases the rate constant for dissociation of vesamicol about 2-fold *despite* a slightly increased equilibrium affinity for vesamicol. The behavior means ATP must induce faster association of vesamicol that compensates for faster dissociation. The significance of the phenomenon is not clear.

The results of this paper lead to the following conclusions. Reorientation of the ACh-binding site in VAChT from the

outside to the inside of vesicles can be observed upon activation of transport. The observation supports the proposed microscopic kinetics model, and it should be useful in characterizing effects of VAChT mutations on the transport cycle (*19*).

ACKNOWLEDGMENT

We thank Dr. Ali Rogani for a gift of rat VAChT cDNA, Dr. Louis B. Hersh for a gift of $PC12^{A123.7}$ cells, and Scott Hauenstein for sequencing recombinant vector.

REFERENCES

1. Bahr, B. A., Clarkson, E. D., Rogers, G. A., Noremberg, K., and Parsons, S. M. (1992) A kinetic and allosteric model for the acetylcholine transporter-vesamicol receptor in synaptic vesicles, *Biochemistry 31*, 5752−5762.
2. Nguyen, M. L., Cox, G. D., and Parsons, S. M. (1998) Kinetics parameters for the vesicular acetylcholine transporter: Two protons exchange for one acetylcholine, *Biochemistry 37*, 13400−13410.
3. Parsons, S. M. (2000) Transport mechanisms in acetylcholine and monoamine storage, *FASEB J. 14*, 2423−2434.
4. Varoqui, H., and Erickson, J. D. (1998) Dissociation of the vesicular acetylcholine transporter domains important for high affinity transport recognition, binding of vesamicol, and targeting to synaptic vesicles, *J. Physiol. 92*, 141−144.
5. Kim, M.-H., Lu, M., Lim, E.-J., Chai, Y.-G., and Hersh, L. B. (1999) Mutational analysis of aspartate residues in the transmembrane regions and cytoplasmic loops of rat vesicular acetylcholine transporter, *J. Biol. Chem. 274*, 673−680.
6. Inoue, H., Li, Y. P., Wagner, J. A., and Hersh, L. B. (1995) Expression of the choline acetyltransferase gene depends on protein kinase A activity, *J. Neurochem. 64*, 985−990.
7. Ojeda, A. M., Bravo, D. T., Hart, T. L., and Parsons, S. M. (2003) in Equilibrium binding and transport studies, *Methods in Molecular Biology* (Yang, Q., Ed.) Vol. 227, pp 155−177, Humana Press, Totowa, New Jersey.
8. Weihe, E., Tao-Cheng, J.-H., Schaefer, M. K.-H., Erickson, J. D., and Eiden, L. E. (1996) Visualization of the vesicular acetylcholine transporter in cholinergic nerve terminals and its targeting to a specific population of small synaptic vesicles, *Proc. Natl. Acad. Sci. U.S.A. 93*, 3547−3552.
9. Bradford, M. M. (1976) A rapid and sensitive method for the quantitation of microgram quantities of protein utilizing the principle of protein-dye binding, *Anal. Biochem. 72*, 248−254.
10. Kornreich, W. D., and Parsons, S. M. (1988) Sidedness and chemical and kinetic properties of the vesamicol receptor of cholinergic synaptic vesicles, *Biochemistry 27*, 5262−5267.
11. Gagliardi, S., Rees, M., and Farina, C. (1999) Chemistry and structure activity relationships of bafilomycin A_1, a potent and selective inhibitor of the vacuolar H^+-ATPase, *Curr. Med. Chem. 6*, 1197−1212.
12. Kessler, R. J., Vande Zande, H., Tyson, C. A., Blondin, G. A., Fairfield, J., Glasser, P., and Green, D. E. (1977) Uncouplers and the molecular mechanism of uncoupling in mitochondria, *Proc. Natl. Acad. Sci. U.S.A. 74*, 2241−2245.
13. Haigh, J. R., Noremberg, K., and Parsons, S. M. (1994). Acetylcholine active transport by rat brain synaptic vesicles, *NeuroReport 5*, 772−776.
14. Varoqui, H., and Erickson, J. D. (1996) Active transport of acetylcholine by the human vesicular acetylcholine transporter, *J. Biol. Chem. 271*, 27229−27232.
15. Zhu, H., Duerr, J. S., Varoqui, H., McManus, J. R., Rand, J. B., and Erickson, J. D. (2001) Analysis of point mutants in the *Caenorhabditis elegans* vesicular acetylcholine transporter reveals domains involved in substrate translocation, *J. Biol. Chem. 276*, 41580−41587.
16. Kim, M.-H., Lu, M., Rogers, G., Parsons, S., and Hersh, L. B. (2003) Specificity of the rat vesicular acetylcholine transporter, *Neurochem. Res. 28*, 473−476.
17. Liu, Y., and Edwards, R. H. (1997) Differential localization of vesicular acetylcholine and monoamine transporters in PC12 cells but not CHO cells, *J. Cell Biol. 139*, 907−916.
18. Krantz, D. E., Waites, C., Oorschot, V., Liu, Y., Wilson, R. I., Tan, P. K., Klumperman, J., and Edwards, R. H. (2000) A phosphorylation site regulates sorting of the vesicular acetylcholine transporter to dense core vesicles, *J. Cell Biol. 149*, 379−395.
19. Bravo, D., and Parsons, S. M. (2002) Microscopic kinetics and structure−function analysis in the vesicular acetylcholine transporter, *Neurochem. Int. 41*, 285−289.

BI049846W